(4*S*)-4-(3-[^{18}F]Fluoropropyl)-L-glutamate

[^{18}F]FSPG

Arvind Chopra, PhD[1]

Created: March 20, 2013; Updated: May 23, 2013.

Chemical name:	(4*S*)-4-(3-[^{18}F]Fluoropropyl)-L-glutamate
Abbreviated name:	[^{18}F]FSPG
Synonym:	[^{18}F]BAY 94-9392
Agent Category:	Compound
Target:	x_c– transporter (sodium-independent anionic amino acid transport system specific for cysteine and glutamate)
Target Category:	Transporter
Method of detection:	Positron emission tomography (PET)
Source of signal / contrast:	^{18}F
Activation:	No
Studies:	• *In vitro* • Rodents • Humans

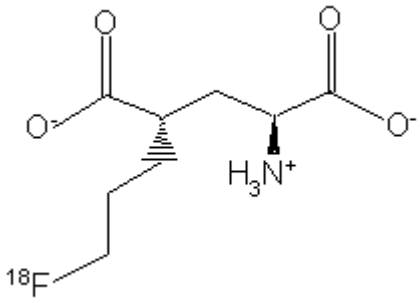

Structure of [^{18}F]FSPG

Background

[PubMed]

The cystine (dimer of L-cysteine)/glutamate antiporter system x_c– is a heterodimeric, sodium-independent, and chloride-dependent anionic amino acid (aa) transporter that transports cystine out of the cell and glutamate into the cell at a ratio of 1:1 (1). In general, the cystine concentration within the cell is very low (because intracellular cystine is rapidly cleaved into two molecules of L-cysteine), and the intracellular concentration of glutamate is relatively higher than in the extracellular spaces. Cysteine is not only a

[1] National Center for Biotechnology Information, NIM, Bethesda, MD 20894; Email: micad@ncbi.nlm.nih.gov.

NLM Citation: Chopra A. (4*S*)-4-(3-[^{18}F]Fluoropropyl)-L-glutamate. 2013 Mar 20 [Updated 2013 May 23]. In: Molecular Imaging and Contrast Agent Database (MICAD) [Internet]. Bethesda (MD): National Center for Biotechnology Information (US); 2004-2013.

component of most proteins; it is also required for the synthesis of glutathione (GSH; a L-γ-glutamyl-L-cysteinyl-glycine tripeptide), an important detoxifier that scavenges and reduces the reactive oxygen or nitrogen species (RO/NS) generated during the metabolic activity of cells (the RO/NS are known to oxidize and denature or modify the activity of proteins, lipids, and DNA in a cell) (2). In addition, GSH influences the intracellular redox signaling pathways during the progression of cell death (2). Therefore, system x_c^- is believed to play an important role in regulating the concentration of GSH in a cell and plays an important role in several physiological processes, such as immune response, inflammation, cellular infection by oncogenic Kaposi's sarcoma herpesvirus, pathogenesis of disorders of the eye (such as age-related macular degeneration) and central nervous system (such as Alzheimer's disease, epilepsy, and cerebral ischemia), growth and progression of cancer, and the development resistance to anticancer drugs by neoplastic cells; for a detailed discussion on the roles of system x_c^- and GSH in health and disease, see Lewerenz et al., and Franco and Cidlowski (1, 2). Many cancerous tissues have a survival advantage over normal cells because they show a higher expression of system x_c^-, accumulate above-normal levels of L-cysteine and L-glutamate, and maintain high levels of GSH to detoxify the RO/NS efficiently (3). Therefore, a variety of inhibitors that target the x_c^- antiporter have been evaluated for drug sensitization or the treatment of cancer (3).

Increased growth and proliferation are the typical characteristics of cancer cells. To maintain these processes, the cells have an increased demand for energy, exhibit increased macromolecules, and metabolize D-glucose and L-glutamine to produce elevated amounts of fatty acids and aa that are required for the survival of the tumor cells (4). There are indications that many tumors do not use the glycolytic pathway and metabolize nutrients such as L-glutamine to produce energy (5). [^{18}F]-Fluorodeoxyglucose ([^{18}F]-FDG), an analog of glucose that is transported into and metabolized similarly to glucose in the cell (after phosphorylation to [^{18}F]-FDG-6 phosphate, it cannot be further metabolized by glycolysis and remains metabolically trapped within the cell), is often used to detect, stage, and monitor cancer therapy with positron emission tomography (PET) [PubMed]. However, a major drawback of PET imaging with [^{18}F]-FDG is that, in addition to tumor cells, normal cells in the brain, heart, brown adipose tissue, etc., also utilize above-average amounts of glucose for energy generation, which can lead to the generation of false-positive results (6). Moreover, it is known that [^{18}F]-FDG imaging cannot always distinguish between infection, inflammation, and tumors (6).

On the basis of the information described above, it was hypothesized that PET agents that target system x_c^- can probably be used to visualize tumors that have an enhanced expression and activity of the antiporter (5). The ^{18}F-labeled structural analog of L-glutamate 4-[^{18}F]fluoro-L-glutamate (BAY 85-8050) was prepared and evaluated with PET for the visualization of tumors in humans (5). *In vitro* studies showed that the labeled compound was transported by both system x_c^- and the sodium-dependent glutamate transporters. In humans, the tumors showed some uptake of the label, but suboptimal PET images were obtained because the labeled compound was defluorinated while it was in circulation (5). Koglin et al. proposed that, to visualize tumors that overexpress system x_c^- with PET, it is necessary to have an agent that is not only metabolically stable but

should interact specifically with the system x_c^- transporter (5). To test this, several ^{18}F-labeled derivatives of L-glutamine were prepared, and it was shown that, among all the ^{18}F-labeled compounds that were evaluated, only (4S)-4-(3-[^{18}F]fluoropropyl)-L-glutamate ([^{18}F]FSPG, [^{18}F]BAY 94-9392) was stable in mouse blood and could be used with PET to visualize tumors that overexpress system x_c^- in mice and rats (5). In clinical studies, it was shown that [^{18}F]FSPG can be used with PET to visualize non-small cell lung cancer (NSCLC) and breast cancer lesions (7), as well as hepatocellular carcinoma (HCC) tumors (8) in humans.

Related Resource Links

Related chapters in MICAD

Amino acid transporters in MICAD

x_c^- transporter in Online Mendelian Inheritance in Man Database (OMIM)

Human x_c^- transporter system in Gene Database. Gene ID: 23657

Protein sequence of human x_c^- transporter

Clinical trials related to amino acid transporters

Synthesis

[PubMed]

The synthesis of nonradioactive FSPG and its labeling with ^{18}F has been described by Koglin et al. (5). The total time taken to synthesize [^{18}F]FSPG was 41–51 min; the radiochemical yield (RCY) and radiochemical purity (RCP) of the final product were 40%–63% and >92%, respectively (as determined with radiographic thin-layer chromatography (TLC; $R_f = 0.46$) and high-performance liquid chromatography). The RCP, RCP, and specific activity of [^{18}F]FSPG used in a clinical study were reported to be 29.1 ± 5.0%, 90.8 ± 0.5%, and >18.2 GBq/μmol (~0.5 Ci/μmol), respectively (7). In another publication, the specific activity of [^{18}F]FSPG at the end of synthesis was reported to be 65.3 ± 15.6 GBq/μmol (1.17 ± 0.42 Ci/μmol) (8).

In Vitro Studies: Testing in Cells and Tissues

[PubMed]

Using competition assays with NIH-H460 lung cancer cells, the IC_{50} values of non-radioactive FSPG against [^{3}H]L-glutamine and [^{3}H]L-cysteine, the natural radiolabeled ligands of system x_c^- transporter, were reported to be 29.1 μmol/L and 33.6 μmol/L, respectively (5). The IC_{50} values for L-glutamine and L-cysteine with these cells were 117.2 μmol/L and 116.4 μmol/L, respectively. This indicated that FSPG had a high specificity of binding for the system x_c^-.

In another study, excess concentrations of L-glutamate, L-cysteine, and p-carboxyphenylglycine (CPG; a specific inhibitor of system x_c^-) were shown to inhibit (~80%) the uptake of [^{18}F]FSPG by the NIH-H460 cells (5). However, no such inhibition was observed with D- or L-aspartate. This again indicated that the uptake of [^{18}F]FSPG in these cells was specifically mediated through system x_c^-.

A TLC analysis of plasma samples obtained at various time points from mice injected with [^{18}F]FSPG showed that the labeled compound remained intact for at least 30 min postinjection (p.i.); later time points were not studied because the tracer was rapidly cleared from circulation (5).

Animal Studies

Rodents

[PubMed]

The biodistribution of [^{18}F]FSPG was investigated in mice bearing NCI-H460 cell tumors (5). The animals (n = 3 mice/time point) were injected with 185 kBq (5 μCi) [^{18}F]FSPG through the tail vein, and the rodents were euthanized at time points ranging from 15 min p.i. to 2 h p.i. All organs of interest were obtained from the animals to determine the amount of radioactivity that accumulated in the various tissues (presented as percent of injected dose per gram tissue (% ID/g)). The uptake of label in the tumors was 4.1± 1.4% ID/g at 15 min p.i. and 3.2 ± 0.4% ID/g at 1 h p.i., and it remained relatively constant thereafter. At 1 h p.i., the tumor/blood and tumor/muscle ratios were 14 and 27, respectively. Among all the tissues, the pancreas showed maximum uptake of the tracer (19.4 ± 4.2% ID/g at 15 min p.i., and uptake decreased to 5.8 ± 0.9% ID/g at 1 h p.i.); all other tissues, including the bone, showed <1% ID/g of radioactivity at 15 min p.i. The presence of a low amount of label in the bone indicated that there was no *in vivo* defluorination of [^{18}F]FSPG (5).

A comparative PET imaging study was performed with [^{18}F]FSPG and [^{18}F]-FDG in nude rats bearing NCI-H460 cell tumors (n = 3 rats/tracer) (5). Identical animal handling and PET imaging protocols were used for both the tracers in this study. The NCI-H460 cell lesions were clearly visible with both [^{18}F]FSPG and [^{18}F]-FDG; with [^{18}F]-FDG, however, high amounts of the label were observed in the muscles, joints, brown fat, and the heart of the animals, in addition to the high levels in the tumor.

Baek et al. evaluated the use of [^{18}F]FSPG with PET to detect human Huh7 liver cancer cell orthotropic tumors in the left liver lobe of Naval Medical Research Institute nude mice (n = 3 animals) (8). The rodents were injected with 7.9–8.3 MBq (0.213–0.224 mCi) [^{18}F]FSPG (route of injection not reported), and micro-PET images of the mice were acquired at 50 min p.i. for 20 min. A low background signal was observed in the liver and other organs of the animals; besides the tumors, the kidneys, and the bladder, only the pancreas and the thymus showed some uptake of the tracer. At 60 min p.i., the uptake of

radioactivity in the tumors was determined to be 4.4 ± 1.3% ID/g, and the tumor/background (T/B) ratio at this time point was 11 ± 1.3.

In another study, the use of [^{18}F]FSPG was evaluated with PET to detect hepatoma MH-3924A cell tumors in the left liver lobe of August-Copenhagen Irish rats (n = 3 animals) (8). The animals were given 7.9–9.1 MBq (0.213–0.245 mCi) [^{18}F]FSPG through an intravenous injection, and micro-PET images of the rats were acquired at 60 min p.i. for 10 min. The pattern of tracer uptake in these animals was similar to that observed in the mouse study described above; the amount of radioactivity accumulated in the tumors was 1.5 ± 0.4% ID/g, and the T/B ratio was 3 ± 2.

From these studies, the investigators concluded that [^{18}F]FSPG can probably be used with PET to detect tumors that overexpress the system x_c^- transporter in rodents (5).

Other Non-Primate Mammals

[PubMed]

No reference is currently available.

Non-Human Primates

[PubMed]

No reference is currently available.

Human Studies

[PubMed]

The use of [^{18}F]FSPG was compared with that of [^{18}F]FDG for the detection of NSCLC tumors (n = 10 patients) and breast cancer tumors (n = 5 patients) that overexpress system x_c^- in humans (7). For [^{18}F]FSPG, each patient was given an intravenous injection of 300 ± 10 MBq (8.1 ± 0.8 mCi; mass dose ≤ 100 μg) of the tracer, and whole-body PET/computed tomographic (CT) images of the individuals were acquired for different time intervals as described elsewhere (7). For PET/CT imaging with [^{18}F]FDG, the patients were given an intravenous injection of 7.4 MBq (0.2 mCi)/kg body weight of the tracer, and whole-body images were acquired as described by Yoon et al. (9). Standardized uptake values (SUV) and the SUV ratios (SUVRs) were calculated from the tumor and blood pool activities as detailed by Baek et al. (7). Using appropriate antibodies, the expression of system x_c^- and CD44 (this antigen stabilizes system x_c^-) in the cancerous lesions of the patients was confirmed with immunohistochemical techniques. In the NSCLC patients, the tumor/blood pool SUVR of [^{18}F]FSPG was similar to that obtained with [^{18}F]FDG (9.7 ± 8.6 *versus* 7.7 ± 4.2); however, this ratio was significantly lower ($P < 0.05$) in the breast cancer patients (3.6 ± 5.4 *versus* 8.9 ± 7.9). [^{18}F]FSPG had sensitivity values of 100% and 60% for the NSCLC tumors (detection of 10out of 10 lesions) and the breast cancer tumors (detection of 3 out of 5 lesions),

respectively, among the cancerous lesions confirmed with immunohistochemistry. In addition, with [^{18}F]FSPG the SUV of the NSCLC lesions correlated significantly ($P < 0.01$) with the immunohistochemical stain intensity of system x_c^- transporter and the CD44 antigen. From these studies, the investigators concluded that [^{18}F]FSPG may be used with PET to detect neoplastic lesions in the NSCLC patients, and that [^{18}F]FSPG can also be used to assess system x_c^- transporter activity in the cancerous lesions (7).

In another study, the use of [^{18}F]FSPG was compared with that of [^{18}F]FDG for the detection of HCC lesions in the patients of this cancer (8). Five patients with HCC that exhibited hyper- or isometabolic lesions with [^{18}F]FDG PET imaging were enrolled to evaluate the tracers. The expression of system x_c^- transporter and the CD44 antigen in the tumors was investigated with immunohistochemistry in 4 out of 5 patients enrolled in the study. The participants were injected with 300 MBq (8.1 mCi) [^{18}F]FSPG, and dynamic whole-body PET scans of the patients were acquired for up to 120 min p.i. PET imaging of the patients showed that [^{18}F]FSPG and [^{18}F]FDG could detect the HCC lesions in 5 out of 5 and 3 out of 5 of the individuals, respectively. Although the SUVRs of tumor/normal liver were comparable for both [^{18}F]FSPG and [^{18}F]FDG (3.6 ± 2.2 *versus* 2.7 ± 1.3), the SUV of the healthy liver was significantly lower ($P < 0.05$) with [^{18}F]FSPG than with [^{18}F]FDG (1.3 ± 0.3 *versus* 1.9 ± 0.2). A moderate or intense accumulation of [^{18}F]FSPG was observed in two of the patients who showed the expression of system x_c^- and the CD44 antigen in the HCC lesions. Lesions of the other two patients did not show expression of the CD44 antigen and had a low uptake of radioactivity from [^{18}F]FSPG. From these studies, the investigators concluded that [^{18}F]FSPG may be suitable for the detection of HCC lesions in the clinic (8).

Supplemental Information

[Disclaimers]

No information is currently available.

References

1. Lewerenz J., Hewett S.J., Huang Y., Lambros M., Gout P.W., Kalivas P.W., Massie A., Smolders I., Methner A., Pergande M., Smith S.B., Ganapathy V., Maher P. *The cystine/glutamate antiporter system x(c)(-) in health and disease: from molecular mechanisms to novel therapeutic opportunities.* Antioxid Redox Signal. 2013;18(5):522–55. PubMed PMID: 22667998.
2. Franco R., Cidlowski J.A. *Glutathione efflux and cell death.* Antioxid Redox Signal. 2012;17(12):1694–713. PubMed PMID: 22656858.
3. Lo M., Wang Y.Z., Gout P.W. *The x(c)- cystine/glutamate antiporter: a potential target for therapy of cancer and other diseases.* J Cell Physiol. 2008;215(3):593–602. PubMed PMID: 18181196.
4. Lieberman B.P., Ploessl K., Wang L., Qu W., Zha Z., Wise D.R., Chodosh L.A., Belka G., Thompson C.B., Kung H.F. *PET imaging of glutaminolysis in tumors by 18F-(2S, 4R)4-fluoroglutamine.* J Nucl Med. 2011;52(12):1947–55. PubMed PMID: 22095958.

5. Koglin N., Mueller A., Berndt M., Schmitt-Willich H., Toschi L., Stephens A.W., Gekeler V., Friebe M., Dinkelborg L.M. *Specific PET imaging of xC- transporter activity using a (1)(8)F-labeled glutamate derivative reveals a dominant pathway in tumor metabolism.* Clin Cancer Res. 2011;17(18):6000–11. PubMed PMID: 21750203.
6. Zhu A., Lee D., Shim H. *Metabolic positron emission tomography imaging in cancer detection and therapy response.* Semin Oncol. 2011;38(1):55–69. PubMed PMID: 21362516.
7. Baek S., Choi C.M., Ahn S.H., Lee J.W., Gong G., Ryu J.S., Oh S.J., Bacher-Stier C., Fels L., Koglin N., Hultsch C., Schatz C.A., Dinkelborg L.M., Mittra E.S., Gambhir S.S., Moon D.H. *Exploratory clinical trial of (4S)-4-(3-[18F]fluoropropyl)-L-glutamate for imaging xC- transporter using positron emission tomography in patients with non-small cell lung or breast cancer.* Clin Cancer Res. 2012;18(19):5427–37. PubMed PMID: 22893629.
8. Baek S., Mueller A., Lim Y.S., Lee H.C., Lee Y.J., Gong G., Kim J.S., Ryu J.S., Oh S.J., Lee S.J., Bacher-Stier C., Fels L., Koglin N., Schatz C.A., Dinkelborg L.M., Moon D.H. *(4S)-4-(3-18F-fluoropropyl)-L-glutamate for imaging of xC transporter activity in hepatocellular carcinoma using PET: preclinical and exploratory clinical studies.* J Nucl Med. 2013;54(1):117–23. PubMed PMID: 23232273.
9. Yoon D.H., Baek S., Choi C.M., Lee D.H., Suh C., Ryu J.S., Moon D.H., Lee J.S., Kim S.W. *FDG-PET as a potential tool for selecting patients with advanced non-small cell lung cancer who may be spared maintenance therapy after first-line chemotherapy.* Clin Cancer Res. 2011;17(15):5093–100. PubMed PMID: 21673067.